Design Considerations and Implementation of Coil Detection and Optimized Switching for a Moving Field Inductive Power Transfer System

Michael Haider*, Mirco H. Metz, Johannes A. Russer, Peter Russer
TUM School of Computation, Information and Technology, Technical University of Munich, Garching, Germany
*michael.haider@tum.de

2024 IEEE-APS Topical Conference on Antennas and Propagation in Wireless Communications (APWC) | 979-8-3503-6077-6/24/$31.00 ©2024 IEEE | DOI: 10.1109/APWC61918.2024.10701723

***Abstract*—Powering electric vehicles with on-road charging capabilities eliminates the need for bulky, expensive batteries and enhances their driving range. This addresses a main limitation of current battery-powered electric vehicles. The proposed Moving Field Inductive Power Transfer system, designed for installation on specific highway segments, enables electric vehicles to recharge intermittently while traveling long distances without the need for dedicated charging stops. The primary coils, operating as switched resonant converters embedded in the road, can hand over energy to the next coil, ensuring a continuous power supply follows the vehicle and its onboard secondary coil. This approach significantly reduces power losses in the road-based charging system. This paper outlines the design considerations and showcases an implementation for optimized handover of energy in a scaled model system.**

***Index Terms*—coil detector (CD), electric vehicles (EV), E|ROAD, moving field inductive power transfer (MFIPT), wireless power transfer (WLPT), zero crossing detector (ZCD).**

I. Introduction

Electric vehicles (EVs) are becoming increasingly widespread and shall replace cars with internal combustion engines (ICE) in the near future. Yet, the cost and weight of the batteries as well as the limited range and comparably long recharging times remain a challenge for battery operated electric vehicles (BEVs). The demand for lithium-ion batteries will increase significantly as further BEVs are replacing ICE cars. While necessary metal resources are available, their mining poses severe environmental concerns. Also an efficient recycling of lithium-ion batteries remains an unresolved problem at this time [1]. The rather short vehicle range and the time consuming charging process pose the greatest technical challenge to BEVs.

The challenge of transporting expensive and heavy batteries in electric vehicles can be addressed with wireless inductive power transfer, as suggested in [2]–[4]. This approach allows for a significant reduction in battery capacity by nearly continuously connecting the vehicle to the power grid, thus eliminating range anxiety. The moving field induction power transfer (MFIPT) concept [5], [6], where power losses are minimized by handing over the stored energy between the primary coils of the resonant converters, enables the use of minimal battery capacities on highways, with batteries then mainly used in local and secondary roads without MFIPT. The system integrates seamlessly into advanced autonomous driving systems utilizing vehicle-to-vehicle (V2V) communication and sensor technologies for collision avoidance, enhancing highway capacities and reducing energy consumption. It is suggested that V2V-equipped autonomous vehicles could more than triple highway capacities [7], making MFIPT systems together with V2V an economical solution for future road traffic. This also encourages a move towards lighter, more sustainable vehicle designs, emphasizing the need for alternatives focusing on energy conservation, environmental friendliness, and resource sustainability. Technological and economic aspects for roadway powering have been studied in [8], [9]. Computer simulations of an MFIPT system show that an efficiency of 95 % can be achieved [8], [10]. The shielding effectiveness of an EV from the magnetic field produced by the MFIPT system inside the car has been considered in [11].

In this paper, we focus on two technical aspects towards the realization of an on-road MFIPT system. The precise detection of the presence of a secondary coil above a primary cell is crucial for efficient wireless power transfer between an MFIPT-equipped road and EVs. The same also holds for stationary charging systems, however, with more relaxed timing constraints. A coil detection circuit needs to provide confirmation for optimal overlap between primary and secondary coils and must also detect undesired metal objects, posing a safety hazard [12]. For MFIPT, besides detecting the overlap between primary and secondary coils, zero-crossing detection plays a crucial role in facilitating energy-efficient dynamic power transfer. The energy distribution in the resonant converter constantly needs to be monitored, such that the hand-over proceedure, discussed in Sec. II, occurs without any losses. We present a design and implementation of a combined zero-crossing and coil detection scheme to hand over energy in a chain of primary converter circuits of an MFIPT system. For demonstration purposes, we have implemented a scaled-down model system providing wireless power delivery of up to 120 W. In the following, we describe the MFIPT system, focusing on implementing zero-crossing and coil detection. Furthermore, we present simulation results and a hardware prototype of the proposed design.

Authorized licensed use limited to: Technische Universitaet Muenchen. Downloaded on December 18,2024 at 11:45:30 UTC from IEEE Xplore. Restrictions apply.

979-8-3503-6077-6/24/$31.00 ©2024 IEEE

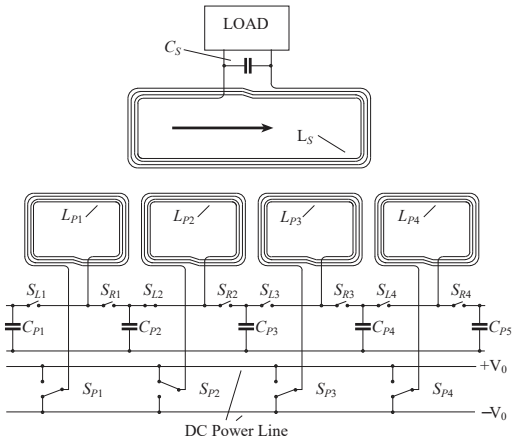

Fig. 1. Moving field inductive power transfer system schematic [10].

II. The MFIPT System

The basic working principle of the MFIPT system [5], [13] is depicted in Fig. 1. The system is based on a series of stationary primary coils linearly arranged along one or multiple tracks on the roadway. The secondary coil is mounted on an EV moving along this track. The fundamental function block of the MFIPT is a resonant converter tuned to a specified operating frequency. It consists of a primary compensation capacitor and a primary coil mounted beneath the surface of the road. Electric vehicles driving along the track are equipped with a secondary coil of at least twice the size of the primary coil [10] to ensure a complete overlap with one active primary coil at any time and an overlap with two primary coils at certain time instances. If the secondary coil overlaps the subsequent primary coil completely, the energy of the first resonant converter cell is transferred to the next one in order to prevent transients and energy losses [5].

The primary coil and the secondary coil, with inductances L_P and L_S respectively, are mutually coupled [13]. The mutual inductance M is given by

$$M = \frac{L_\mathrm{tot} - (L_\mathrm{P} + L_\mathrm{S})}{2}\,. \tag{1}$$

Here, the total inductance L_tot is obtained by connecting one port of the primary coil to one port of the secondary coil and measuring the inductance at the two remaining ports. A coupling coefficient k with $k \in [0, 1]$ is defined as

$$k = \frac{M}{\sqrt{L_\mathrm{P} L_\mathrm{S}}}\,. \tag{2}$$

Consider the wireless power transfer cell L_P2-C_P2 in Fig. 1 to be the initial cell which interacts with the secondary resonant tank L_S-C_S while the switch S_L2 is closed and S_P2 is toggling between $+V_0$ and $-V_0$. Switches of type S_P are implemented with H-Bridges which are connected to a positive-only DC rail corresponding to $+V_0$ in Fig. 1. The detection of the overlap of L_P3 is handled by a coil detector (CD) which signals an incoming secondary coil to the control circuitry which then starts the energy handover and powering process of the next primary cell. The switch S_R2 is closed as soon as the capacitor C_P2 is discharged completely and at the same moment, the switch S_L2 is opened. A zero-crossing detector (ZCD) is implemented to give precise information about the time instance when the primary capacitor is reaching the value of $0\,\mathrm{V}$. At this point, the secondary resonant circuit is interacting with the resonant circuit L_P2-C_P3. If the primary coil L_P2 has a current flow of $0\,\mathrm{A}$, the switch S_L3 is closed and immediately after this the switch S_R2 is opened. Now the subsequent primary resonant circuit is interacting.

III. Handover Between Primary Cells

To facilitate precisely timed switching, exact knowledge about the time delays in the circuitry is important to determine the best instance of time for replacing the reactive elements. While we are presenting a scaled down demonstrator here, we also want to give considerations for the required switching times for a full sized realistic MFIPT scenario. The transit time t_T for an EV moving with a velocity of $v = 130\,\mathrm{km/h} \cong 36\,\mathrm{m/s}$ provides the duration of a full overlap of the secondary coil with a single primary coil. If we assume a primary coil length of $1\,\mathrm{m}$ and a secondary coil of double the length in the EV, the transit time $t_\mathrm{T} \approx 30\,\mathrm{ms}$. The detectors should be able to deliver precise and replicable information on the timing when a primary coil and the secondary coil have complete overlap and when the voltage of the primary compensation capacitor C_P or the current of the primary coil L_P that is currently active in terms of resonant conversion has reached the zero level. Hence, we have to detect a full coil overlap between primary and secondary coil first. If this condition is met, switching needs to be performed such that the compensation capacitor of the next primary cell is activated and the currently active cell's capacitor is separated at a time when all energy is stored in the coil. Switching to the next coil, in turn, takes place when all energy is stored in the capacitor. The task of sensing coil overlap is performed by the CD, while the task to find the ideal timing for switching to the next reactive elements is performed by the ZCD.

A. The Coil Detector

The CD determines whether or not the secondary coil is located above the subsequent primary coil. A full overlap of the primary and secondary coils is achieved, when the coupling factor k is maximum. In our design studies it proved that implementing a CD by monitoring the induced voltage of the deactivated primary coil was not viable since it was not proportional to the increasing coupling factor k at all times. Hence, stability and reliability of the detection circuit was compromised. Instead of measuring the open loop voltage of the coil, one could also load the primary coil with a known resistor and monitor the voltage drop at the resistor. While the latter approach prevented voltage fluctuations and resulted in a satisfactory proportionality relation between the measured voltage and the coupling coefficient k, the approach has a

Authorized licensed use limited to: Technische Universitaet Muenchen. Downloaded on December 18,2024 at 11:45:30 UTC from IEEE Xplore. Restrictions apply.

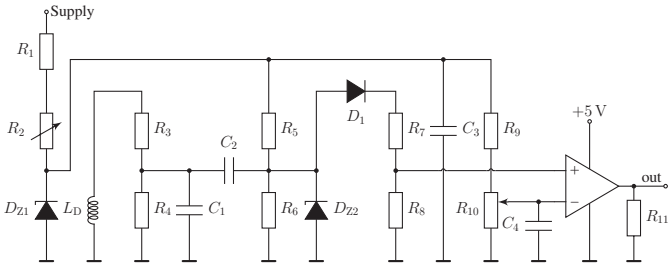

Fig. 2. Basic circuit for coil detection as well as zero-crossing detection.

major drawback: Energy losses are enormous and the resistor has to be disconnected while the primary coil is active.

Finally, we decidet to use an additional coil separate from the primary coil for the CD. The CD circuit is depicted in Fig. 2.

Instead of a multi-turn detection coil, we simulated a single turn CD, which gave very good detection properties and an energy loss significantly lower than $1\,\%$ (in the range of $15\,\mathrm{mW}$). An LT1719 [14] operational amplifier was chosen as a comparator in Fig. 2. The supply voltage is connected to a fixed resistor R_1 and a variable resistor R_2. These ensure an appropriate current through the precision micropower shunt voltage reference diode D_{Z1}, realized by a LM4040-10 [15], which has an output voltage of $10\,\mathrm{V} \pm 10\,\mathrm{mV}$, stabilized by C_3. The reference voltage is then divided by the resistor R_9 and a high precision potentiometer R_{10}, and stabilized by a small capacitor C_4 which leads to a precise voltage reference for the inverting input of the operational amplifier. The voltage ripple is around $500\,\mu\mathrm{V}$. The single turn detection coil is denoted as L_D in Fig. 2. The voltage induced in L_D is divided by R_3 and R_4 and filtered with a high-frequency noise-canceling capacitor C_1. Then, the capacitor C_2 blocks any DC currents. The operating point is adjusted such that the signal is overlaped by a defined DC offset generated by the voltage divider R_5 and R_6. The diode D_1 blocks negative voltages and the Zener diode D_{Z2} has a breakdown voltage of $6.8\,\mathrm{V}$. The final voltage divider in this circuit consisting of R_7 and R_8 with a ratio of $1:1$.

In general, the threshold voltage for coil detection depends on the load condition in the secondary circuit. Thus, maintaining a constant load resistance at the secondary side is crucial for reliable coil detection. The threshold voltage can be adjusted by the precision potentiometer R_{10}. If,however, the threshold voltage is lowered, the probability of false detection will eventually rise which could yield unexpected behavior of the CD output. We simulate the noninverting operational amplifier input voltage V_in, which is equal to the voltage across the resistor R_8 in Fig. 2, for a fixed load resistance of $18\,\Omega$. Then, we vary the coupling factor k in order to determine the behavior of the CD if value of k goes outside of the previously specified region, determining the threshold. In Fig. 3, we can see that the CD will click at a k value of at least 0.29. This is not a coincidence since in our circuit design and simulation of the CD, we assumed $k = 0.3$ for a complete overlap of primary

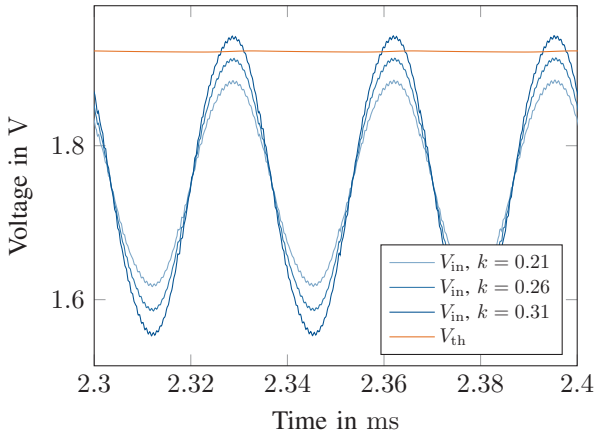

Fig. 3. Coil detector input voltage V_in at R_8 (Fig. 2) for different k values ($R_\mathrm{load} = 18\,\Omega$). The threshold voltage is given in orange.

and secondary coils. If the secondary coil starts to overlap the subsequent primary coil $L_{\mathrm{P}3}$, we initially find $k = 0.21$ and shortly after, the value rises to $k = 0.29$ once the coil $L_{\mathrm{P}3}$ is overlaped by around $95\,\%$ for our chosen coil specifications and arrangement.

B. The Zero-Crossing Detector

For the ZCD, an implementation with a through-wire current sensor was considered. It proved to be advantageous to make use of similarities in the design requirements of the ZCD as compared to the CD. A design with a through-wire current sensor in which the input voltage is compared to ground turned out to pose additional challenges when dealing with negative voltages at the comparator input. Therefore the CD circuit from Fig. 2 was taken as a basis and was modified for the task of zero-crossing detection. We use a Murata 56100C [16] current sensing transformer. The high-frequency filtering capacitor C_1 from Fig. 2 was discarded as high-frequency noise was not found to be an issue here. The noise is most possibly being suppressed by the current transformer or the modified voltage divider.

The ZCD should be able to cope with different k values, which was verified by simulations in order to ensure an output voltage with low time jitter for a fixed load resistance. The coupling coefficient k is assumed to remain constant during the time period when the ZCD is operated. Nevertheless, it is important to know the behavior of the circuit if something unexpected happens. This could be, e.g., an obstacle on the road, a bump within the road, or simply if the EV has an off-standard distance between primary and secondary coils. The output current of the ZCD along with the voltages at the primary capacitor obtained for different k values are shown in Fig. 4. We have observed a time jitter of smaller than $\pm 25\,\mathrm{ns}$, which is a very good value in order to determine the right switching instances precisely.

IV. Hardware Implementation

The primary coils of the demonstrator are designed to transfer power of up to $120\,\mathrm{W}$ with a primary current

Authorized licensed use limited to: Technische Universitaet Muenchen. Downloaded on December 18,2024 at 11:45:30 UTC from IEEE Xplore. Restrictions apply.

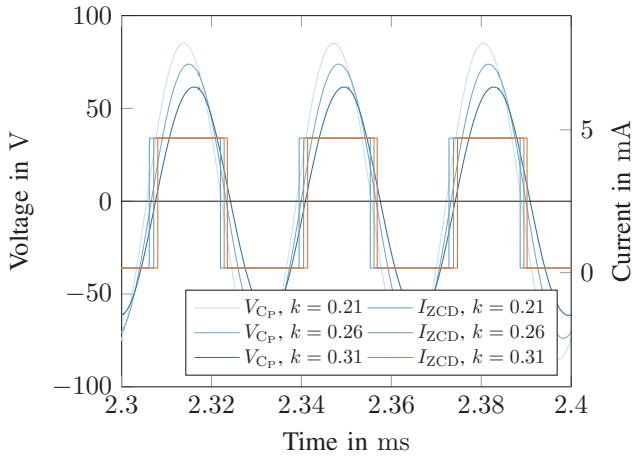

Fig. 4. Voltage in the primary capacitor V_{C_p} and current in the ZCD output resistor R_{11} (Fig. 2) for different k values.

of up to 30 A. Ill-timed switching will easily cause high self-induced voltages in the range of a few kilovolts within the coils, causing destruction of the circuit. Therefore, dedicated transient voltage suppressor (TVS) diodes protect the remaining circuitry. A finite state machine for detection and switching is implemented in the control circuit in terms of a microcontroller with interrupts. An image of the demonstrator featuring three primary cells, along with the power, switching, detection, and control circuits can be seen in Fig. 5. Each unit cell circuit features dedicated 'shutdown' and 'run' pins in order to save energy by turning off primary cells that are currently not actively needed. Since the start-up and wake-up time of all chips is less than 5 ms, an EV would have to drive with a speed of more than 300 km/h to be faster than the initialization process of the subsequent control circuit.

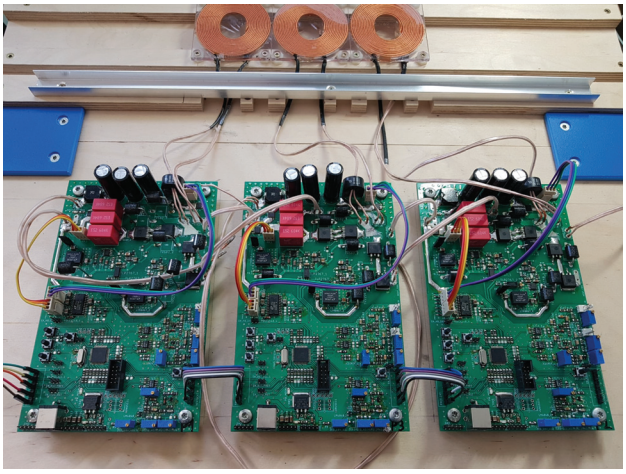

Fig. 5. Prototype of the powering, switching, and control circuitry and primary coils.

V. Conclusion

In this work, a CD and a ZCD for an MFIPT system were presented. Circuits have been developed and design considerations were discussed. The detectors were implemented along with control circuitry for a scaled MFIPT demonstrator system. The detectors provide relevant timing information to operate a MFIPT system with optimized efficiency. Both, the CD and the ZCD are protected from voltage spikes and negative voltage levels to ensure maximum stability in the testing process without destroying the sensitive devices.

References

[1] D. Castelvecchi, "Electric cars and batteries: How will the world produce enough?" *Nature*, vol. 596, no. 7872, pp. 336–339, 2021.
[2] J. G. Bolger, L. S. Ng, D. B. Turner, and R. I. Wallace, "Testing a prototype inductive power coupling for an electric highway system," in *29th IEEE Vehicular Technology Conf.*, vol. 29, 1979, pp. 48–56.
[3] M. L. G. Kissin, J. T. Boys, and G. A. Covic, "Interphase mutual inductance in polyphase inductive power transfer systems," *IEEE T. Ind. Electron.*, vol. 56, no. 7, pp. 2393–2400, 2009.
[4] O. Olsson, "Slide-in Electric Road System, Inductive project report, Phase 1," Scania CV AB, 2013. [Online]. Available: http://urn.kb.se/resolve?urn=urn:nbn:se:ri:diva-26026
[5] J. A. Russer and P. Russer, "Design considerations for a moving field inductive power transfer system," in *Proc. IEEE Wireless Power Transfer Conf. (WPTC)*, 2013, pp. 147–150.
[6] P. Russer, "Verfahren und Anordnung zur drahtlosen Energieübertragung," DE Offenlegungsschrift DE 10 2013 000 900 A1, Jul. 24, 2014.
[7] P. Tientrakool, Y.-C. Ho, and N. F. Maxemchuk, "Highway capacity benefits from using vehicle-to-vehicle communication and sensors for collision avoidance," in *IEEE Vehicular Technology Conference (VTC Fall)*, 2011, pp. 1–5.
[8] J. A. Russer, M. Haider, M. Weigelt, M. Becherer, S. Kahlert, C. Merz, M. Hoja, J. Franke, and P. Russer, "A system for wireless inductive power supply of electric vehicles while driving along the route," in *7th Int. Electric Drives Production Conf. (EDPC)*, 2017, pp. 1–6.
[9] M. Weigelt, A. Mayr, M. Masuch, K. Batz, J. Franke, P. M. Bican, A. Brem, J. Russer, and P. Russer, "Techno-economic evaluation of strategic solutions to extend the range of electric vehicles," in *8th Int. Electric Drives Production Conf. (EDPC)*, 2018, pp. 1–7.
[10] J. A. Russer, M. Dionigi, M. Mongiardo, and P. Russer, "A moving field inductive power transfer system for electric vehicles," in *European Microwave Conf.*, 2013, pp. 519–522.
[11] M. Haider and J. A. Russer, "Field modeling of dynamic inductive power supply of electric vehicles on the road," in *Int. Conf. Electromagnetics in Adv. Appl. (ICEAA)*, 2017, pp. 1490–1493.
[12] H. Zhang, D. Ma, X. Lai, X. Yang, and H. Tang, "The optimization of auxiliary detection coil for metal object detection in wireless power transfer," in *IEEE PELS Workshop on Emerging Technologies: Wireless Power Transfer*, 2018, pp. 1–6.
[13] A. Costanzo, M. Dionigi, F. Mastri, M. Mongiardo, G. Monti, J. A. Russer, and P. Russer, "The basic cell operating regimes for wireless power transfer of electric vehicles," in *IEEE Wireless Power Transfer Conf. (WPTC)*, 2016, pp. 1–4.
[14] Linear Technology Corporation, "LT1719 - 4.5ns Single - Dual Supply 3V - 5V Comparator with Rail-to-Rail Output," Analog Devices, Norwood, MA, USA, pp. 1–22, 2000.
[15] National Semiconductor Corporation, "Precision Micropower Shunt Voltage Reference," National Semiconductor Corporation, Santa Clara, CA, USA, pp. 1–30, August 2002.
[16] Murata, "5600 Series 10 A Current Sensing Transformers," Murata, Yokohama, Kanagawa, Japan, pp. 1–2, 2012.

Authorized licensed use limited to: Technische Universitaet Muenchen. Downloaded on December 18,2024 at 11:45:30 UTC from IEEE Xplore. Restrictions apply.